Radiation Measurements 47 (2012) 201–209

Contents lists available at SciVerse ScienceDirect

Radiation Measurements

journal homepage: www.elsevier.com/locate/radmeas

Application of pulsed OSL to polymineral fine-grained samples

James K. Feathers [a,*], M. Aksel Casson [a], Amanda Henck Schmidt [b], Makaiko L. Chithambo [c]

[a] Department of Anthropology, University of Washington, Box 353100, Seattle, WA 98195-3100, USA
[b] Department of Earth and Space Sciences, University of Washington, Box 351310, Seattle, WA 98195-1310, USA
[c] Department of Physics and Electronics, Rhodes University, PO Box 94, Grahamstown 6140, South Africa

ARTICLE INFO

Article history:
Received 17 June 2009
Received in revised form
10 May 2011
Accepted 10 January 2012

Keywords:
Pulsed OSL
Fine-grained luminescence dating
Anomalous fading
Alpha efficiency
Chinese terracettes

ABSTRACT

Pulsed OSL is applied to nine fine-grained sediment samples from Sichuan province, China, using stimulating pulses of 10 μs on and 240 μs off, with an infrared exposure prior to each OSL measurement. Comparison of fading rates between pulsed and non-pulsed signals, the latter also obtained with a preceding IR exposure, shows that fading is significant for mainly the non-pulsed signals. Presence of a pulsed IRSL and the magnitudes of *b*-value to correct for lower alpha efficiency suggest that pulsing does not fully remove a significant feldspar signal, only a fading component. Comparison with ages of quartz extracts shows that pulsed OSL ages are consistent, while CW-OSL ages are slightly older and CW-IRSL ages are much older. The older ages suggest a less well-bleached feldspar component.

© 2012 Elsevier Ltd. All rights reserved.

1. Introduction

Luminescence dating commonly uses 100–200 μm grains of quartz or feldspars as dosimeters, but many samples – both sediments and ceramics – lack coarse grains, and from early on an alternative dating method using fine grains (<15 microns) has been offered (Zimmerman, 1967). Aside from providing a means to date fine-grained samples, the method has other advantages. Because such fine grains do not attenuate alpha radiation, the alpha dose rate makes up a large portion of the total dose rate, reducing the proportional contribution from gamma radiation, the dose rate from which can be difficult to estimate in complicated environments.

Dating of fine grains has two principle disadvantages. One is that because of difficulties in isolating particular minerals with relatively well-known luminescence properties, fine-grain samples are usually polymineral and therefore can contain components with undesirable luminescence properties. The main concern involves components that suffer from anomalous fading, particularly feldspars, which because they have bright signals may dominate the total signal. Polymineral signals may also include contributions from minerals such as micas, whose luminescence properties are poorly known (Kortekaas and Murray, 2005). The second problem is the low efficiency of alpha irradiation at producing luminescence. This varies for different minerals and is often hard to measure precisely. Other potential problems come to mind as well. Signals from alpha irradiation may behave differently, e.g., fading at different rates, than signals from beta or gamma irradiation (Visocekas, 1988). The short range of alpha particles may also produce inhomogenous dose rate effects, for example in respect to water content, that may increase uncertainty in the date obtained. These latter issues remain unexplored.

After the development of an OSL single-aliquot method for deriving equivalent dose (D_e) from coarse-grained quartz (Murray and Wintle, 2000), several researchers (Banerjee et al., 2001; Roberts and Wintle, 2001) attempted to apply a modified version to fine-grained material in such a way as to remove the feldspar or fading component. Dubbed "double SAR", the method involves an infrared exposure to the sample prior to each OSL measurement (now commonly employing blue-light stimulation). Because feldspar signals are reduced by infrared exposure but quartz signals are not (except at higher temperatures), the subsequent OSL signal derives mainly from quartz (and perhaps other minerals). However, feldspars are also sensitive to blue-light stimulation. Duller and Bøtter-Jensen (1993) argue that separate traps, one sensitive to blue/green stimulation and the other sensitive to both blue/green and IR, are involved. This does not guarantee that an IR exposure will reduce the feldspar signal to an insignificant level. Experience with the method has shown that in some cases a feldspar signal does remain (Roberts, 2007). Efforts have been made to further reduce the feldspar signal by prolonged IR exposure (Zhang and Zhou, 2007), or to eliminate feldspars completely by chemical treatment during sample preparation (Roberts, 2007). The latter

* Corresponding author. Tel.: +1 206 685 1659; fax: +1 206 543 3285.
E-mail address: jimf@u.washington.edu (J.K. Feathers).

1350-4487/$ – see front matter © 2012 Elsevier Ltd. All rights reserved.
doi:10.1016/j.radmeas.2012.01.003

has employed hydrofluorosilicic acid (H_2SiF_6), but the high cost of this particular chemical makes routine use expensive.

Recent research with coarse-grained materials has shown that pulsed OSL can be used to reduce a contaminating feldspar signal from quartz extracts. In pulsed OSL the luminescence signal is collected through a series of pulses with the stimulating light alternatively turned on and off. The time duration between stimulation and emission for the main component of feldspar is much shorter than that of quartz (Sanderson and Clark, 1994; Clark et al., 1997; Bailiff and Mikhailik, 2003; Chithambo, 2007a,b; Denby et al., 2006), suggesting that if the signal is collected only after the stimulating light is turned off, a properly selected pulse width can discriminate against a feldspar signal, excepting some longer, low intensity components in feldspar. Thomsen et al. (2006, 2008a) using pulses from blue (470 nm) stimulation of 50 μs on and 50 μs off, not only reduced the feldspar signal during the off-time, but also found that the feldspar signal could be further reduced if each blue stimulation is preceded by an IR exposure (870 nm). Experiments by Ankjaergaard et al. (2010) have suggested the best separation of quartz from a mixed signal can be achieved with on- and off-time settings of 50 μs each or 20 μs on- and 80 μs off-time, again including a preceding IR exposure. In this paper, we extend the use of pulsed OSL to fine-grained samples.

2. Samples

We collected nine sediment samples from hillside terraces surrounding Jianpan Village in Jiuzhaigou National Park in northern Sichuan, China (Fig. 1, Table 1), as part of a multi-disciplinary study by Sichuan University, the national park, and the University of Washington (Henck et al., 2010). Large quantities of archaeological materials, including stone structures, pottery and stone tools, have been found eroding from the face of the terraces. The terraces are of varied size, ranging in height from 1 to 50 m, in width from 2 to 100 m, and in length up to 500 m. They are irregular in shape and run approximately parallel to the hillside contours. In other places similar, but generally smaller formations have been called terracettes and the process by which they are formed has been debated at

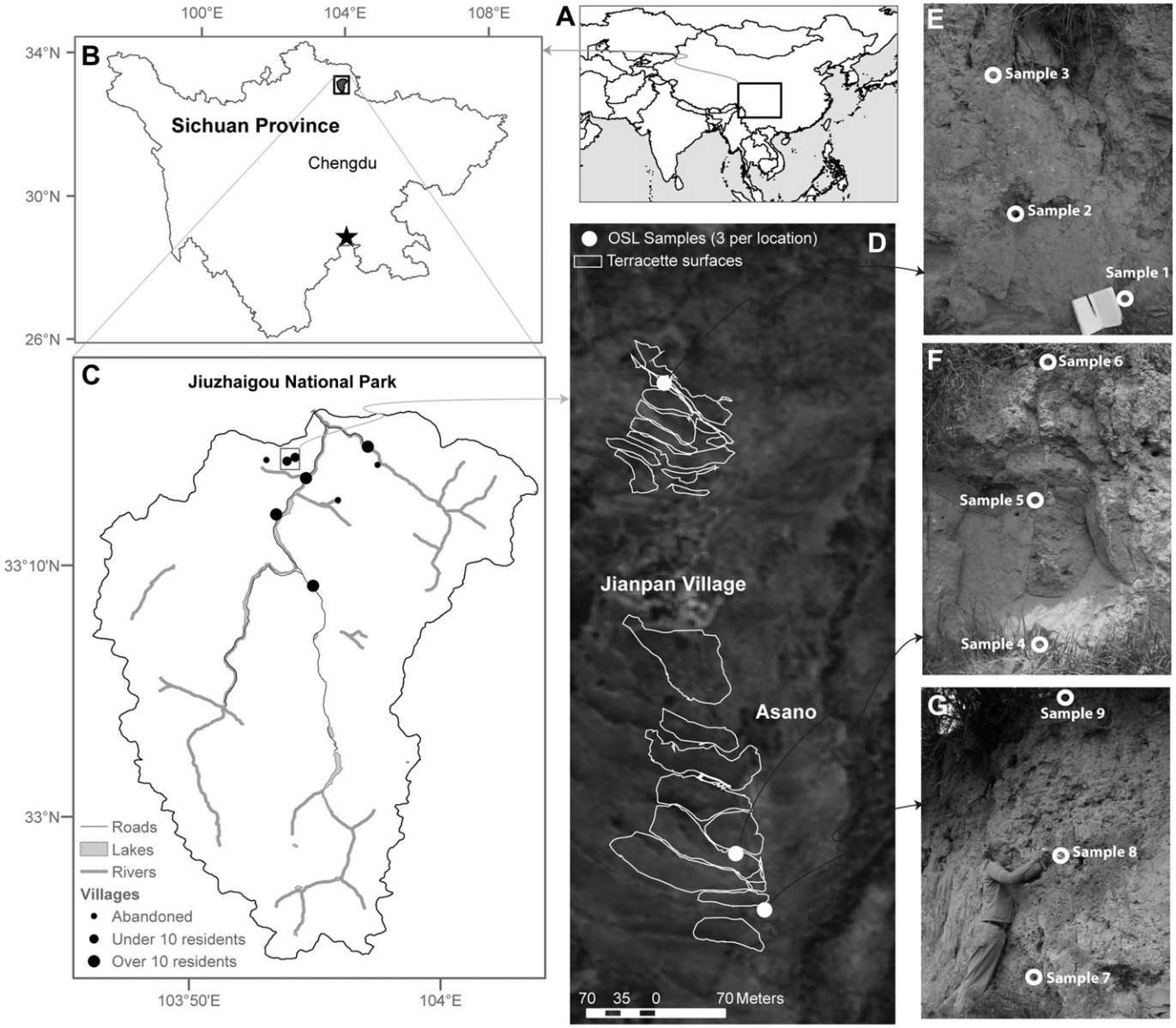

Fig. 1. Location of samples. Three samples were taken from the profiles of three different terracettes. Samples were collected by Amanda Henck, shown in the lower right.

Table 1
Samples from Jianpan Village, Sichuan, China. See Fig. 1 for locations.

Laboratory #	Sample #	Depth from surface (m)
UW1691	1	2.0
UW1692	2	1.5
UW1693	3	0.5
UW1694	4	4.0
UW1695	5	2.0
UW1696	6	0.5
UW1697	7	6.0
UW1698	8	4.0
UW1699	9	0.5

length, with explanations ranging from landslides to erosional effects from grazing (Vincent and Clarke, 1979).

The sediments in the Jiuzhaigou terraces are composed of fine-grained loess-like silt. Stratigraphy exposed in the terrace faces often shows a distinct paleosol separating artifact-containing strata from younger strata, which are either landslide or loess-like deposits. While we do not know the exact formation mechanism for the terraces, the artifacts and ethnographic evidence suggest an anthropogenic origin from local swidden agricultural practices. We interpret the paleosol to be a former plow surface that was subsequently buried by landsliding, probably at the time the village was abandoned. The sediments probably originated as wind-blown silts, but then likely underwent slumping during terrace formation. The archaeological evidence suggests that the slumps pre-date the paleosol as the houses are parallel to the modern surface (Henck et al., 2010).

Slumping involves minimal sunshine exposure, so the dates may address the original aeolian deposition, in which case they should be well bleached. They should also retain the original stratigraphic order, so that ages should increase with depth. An exception might be where surfaces were exposed long enough to develop a soil. During this time partial bleaching is likely through plowing, which does not turn over the soil in a uniform manner. Similarly, sediments in landslide deposits may also be partially bleached as some landslide processes could expose some, but not all, sediments to sunlight.

3. Procedures

Sediments were collected in light-tight cylinders driven into the terrace faces. Exposed ends were removed in the laboratory in subdued red–orange light. Samples were first treated with HCl and H_2O_2 to remove carbonates and reduce organics. The 1–8 μm fraction from each sample was isolated by suspending grains in acetone for 2 and 20 min, retaining the supernatant after the former and the sediment on the bottom after the latter. The 20-min settling was done at least twice to insure all grains <1 μm were removed. The suspended 1–8 μm fraction was then settled onto 1 cm stainless steel disks by evaporation of the acetone at 50 °C. On six samples, a portion of the 1–8 μm fraction was treated with quartz-buffered H_2SiF_6 following procedures of Roberts (2007). Subsequent luminescence measurements of this material showed no signal above background when exposed to infrared light. These measurements provide a way to evaluate the efficacy of pulsed OSL for reducing a feldspar signal.

Luminescence was measured on Risø reader DA-20. Blue (470 nm) and infrared (870 nm) diodes were used for stimulation, while emission was through 7.5 mm Hoya U-340 filters (UV). Double SAR procedures for equivalent dose (D_e) determination used five regeneration doses, a zero dose and a repeat of the first regeneration dose. A preheat of 240 °C for 5 s, a test dose of about 3 Gy, and a cutheat of 200 °C were employed. In conventional continuous wave (CW) mode, IRSL was measured for 100 s at 60 °C, followed by OSL measured for 100 s at 125 °C.

Pulsed measurements were carried out using an attachment to the DA-20, consisting of a microcontroller with a programmable, hardware-controlled timer and a solid state switch for pulsing (Denby et al., 2006). The signal while the stimulating light is on is gated off, so that only the signal when the stimulating light is off is collected. The gating circuit provides a counting window that permits the signal after each pulse to be accumulated and plotted against exposure time as a decay curve. Time resolved spectra, where counts from both on- and off-time are summed over many pulses as a function of time between stimulation and emission, were not processed. With the equipment used in this paper, pulsed mode and the timing of the pulses are set up manually and it is neither possible to switch back and forth between pulsed and CW stimulations within the same double SAR sequence, nor change the time settings during the sequence. Because pulsed measurements take considerable machine time and adding additional CW exposure at the end of each step is not possible, only shorter pulsed exposures are practical on a routine basis and thus concern arises as to whether OSL exposure at each step is sufficient to reset the signal.

The pulse width was set for 10 μs on and 240 μs off. This was based on an early recommendation from Christina Ankjaergaard (personal communication), although her more recent work (Ankjaergaard et al., 2010) has suggested that longer on-times and shorter off-times, and thus reduced measurement time, can be effective. However, our samples are relatively insensitive, and to improve our signal the shorter on-time was an effective choice even if the separation between quartz and feldspar was not optimal. From consideration of quartz luminescence lifetimes (related to the delay between stimulation and emission), we deduced that at least 60% of the quartz signal is emitted after 10 μs (Chithambo, 2007b). To save machine time, most measurements were made for 100 s. This amount of time allows 400,000 pulses, which is equivalent to 4 s of continuous wave exposure. While probably sufficient to reset the fast component in quartz, we worried about sufficient exposure to reset, particularly, the feldspar component. Therefore, comparison measurements on three samples were made using measurement times of 1000–1200s (effective 40–48s exposures). All comparisons between pulsed and CW signals used the same integrated stimulation time (i.e., on-time) for both signal (initial 1.2 s) and background (2.8–4 s).

The beta source attached to the Risø unit was calibrated for stainless steel disks using 1–8 μm quartz. The quartz was obtained by crushing three coarse-grained (90–212 μm) samples known to consist of almost 100% quartz. After crushing, the grains from each sample were irradiated at Pacific National Laboratory, Hanford, WA, in 2.3 mm thick glass tubing with 3.0, 5.9, or 9.2 Gy of ^{60}Co gamma radiation at a distance of 100 cm and with an uncertainty of 2.3%. Calibration, using SAR protocol on 18 aliquots, yielded an average value of 0.120 ± 0.003 Gy/s.

Fading was monitored by employing an anomalous fading test for both pulsed and CW signals, following single-aliquot procedures of Auclair et al. (2003). Any fading corrections followed Huntley and Lamothe (2001). Alpha efficiency was measured using the *b*-value system (Huntley et al., 1988). The *b*-value was obtained in several ways for different samples: adding alpha doses with beta test doses to the SAR procedure; performing a full SAR sequence using some alpha and some beta regeneration points and using both alpha and beta test doses at each step; performing separate SAR procedures, one using betas and one using alphas for both regeneration and test doses, on separate aliquots; and administering an alpha dose prior to an SAR sequence using beta doses (Lai,

2008). In all cases the *b*-value was taken as the ratio of the beta equivalent dose (in Gy) to the alpha equivalent dose (in μm^{-2}). No systematic differences were found for any of the methods, but precision varied greatly. Alpha irradiation was administered both by a Littlemore stand-alone alpha irradiator and an alpha source attachment to the DA-20. The strength of the Littlemore alpha source is $0.143 \pm 0.005\ \mu m^{-2}/m$. An attempt to calibrate the DA-20 source against the Littlemore source yielded uncertainties 2–3 times greater. Averages given in the next section are weighted by precision, so that results from the Littlemore irradiator predominate.

Dose rates were measured by a combination thick source alpha counting, thick source beta counting and flame photometry. No on-site dosimetry was possible.

4. Results

Fig. 2a shows decay curves for 40 s exposures from two different polymineral, fine-grain aliquots of UW1691 and from one fine-grain quartz aliquot of UW1697. Time on the *x*-axis is "on-time", which would be equivalent to continuous wave time. One can see that the decline of the pulsed OSL is similar to that of the quartz

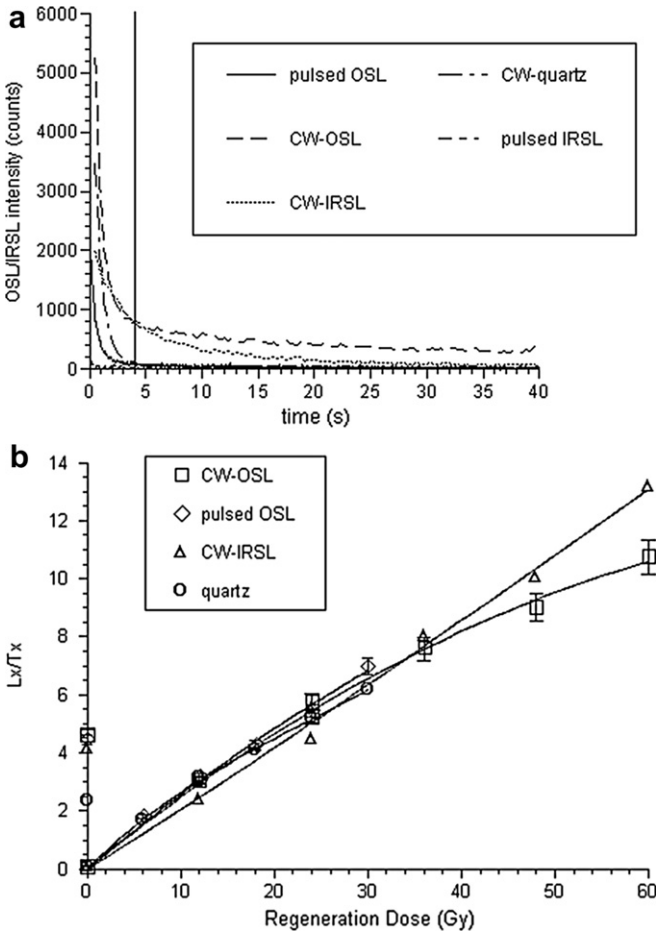

Fig. 2. (a) Decay curves using continuous wave and pulsed OSL over 40 s for two different polymineral aliquots of UW1691, and using continuous wave OSL for a fine-grained quartz aliquot of UW1697. The quartz signal is divided by 10 for comparative purposes. Time is "on-time", in other words "equivalent continuous wave time". The vertical line represents the limit of a 4-s exposure. (b) Growth curves for the same aliquots. The regenerations doses for the pulsed OSL and the quartz curves were half those of CW for the same step in the SAR sequence. Symbols above the origin on the *y*-axis represent the natural signal.

Table 2
Comparison of equivalent dose (D_e) and over-dispersion (σ_b) values for different pulsed exposures.

Sample	4 s exposure			40–48 s exposures		
	N	D_e (Gy)	σ_b (%)	N	D_e (Gy)	σ_b (%)
UW1691	8	19.4 ± 0.5	5.2 ± 2.6	9	17.9 ± 0.5	6.6 ± 2.6
UW1694	8	50.1 ± 4.2	17.6 ± 7.1	9	52.0 ± 2.8	9.7 ± 5.8
UW1699	3	2.0 ± 0.6	0	5	1.6 ± 0.3	27.9 ± 13.7

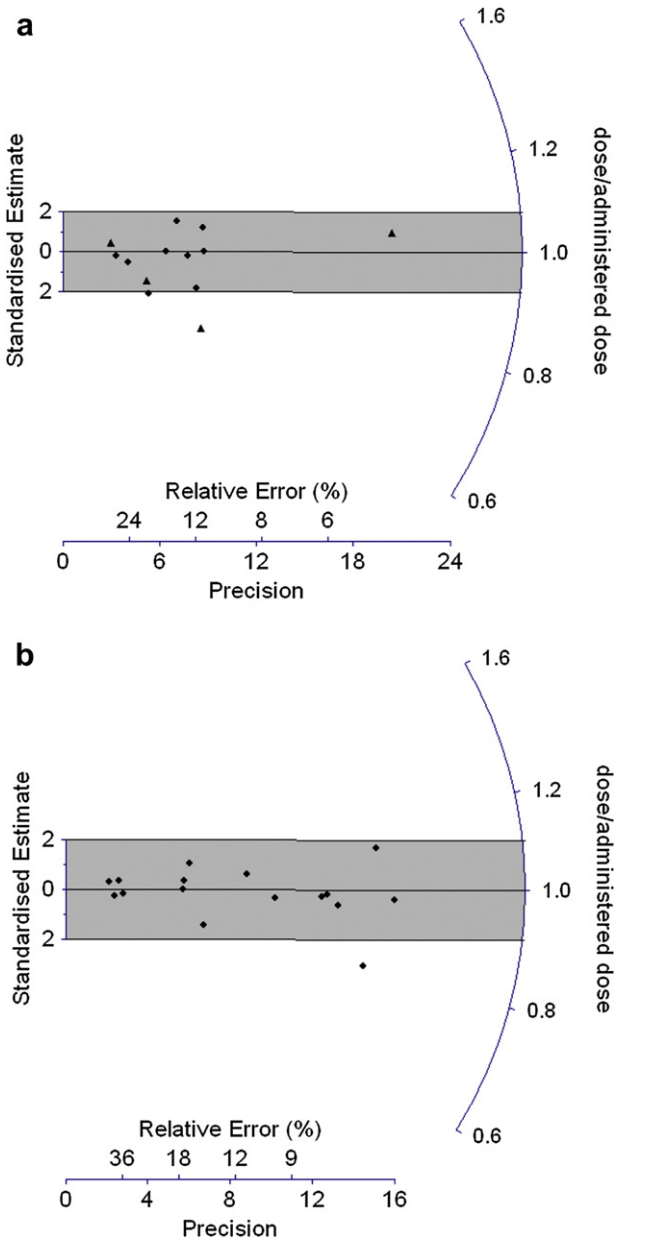

Fig. 3. (a) Radial graph showing dose recovery results for 4 s (diamonds) and 40 s (triangles) exposures for pulsed OSL. Plotted on the *y*-axis are ratios of administered to recovered dose, standardized by the number of standard deviations from 1. Precision is plotted on the *x*-axis. Lines drawn from the origin through any point intersect the right-hand scale at the measured value. (b) Radial graph showing dose recovery test for continuous wave OSL. Signals used for these and other single-aliquot values used the same integrated on-time signal (whether exposed for 4 or 40 s). Errors reflect counting statistics, regression fits, and a 2% instrumental error.

sample. The CW-OSL curve declines nearly as rapidly and must be dominated by a fast-decaying component, while the CW-IRSL declines at a slower rate. A pulsed IRSL signal is barely present. Fig. 2b shows growth curves for the same aliquots (except for pulsed IRSL, which for this aliquot had no measurable growth curve). They vary little, except at higher doses where the CW-OSL signal begins to saturate (the quartz OSL growth curve was not carried out as far).

Table 2 compares D_e values from pulsed measurements on aliquots subject to 4 or 40–48 s exposures for three samples covering the range of D_e magnitudes. Aliquots using 40 or 48 s exposures showed no significant difference so these results are combined in the table. The analyzed signal is the first two 1.2 s, and the background is 2.8–4 s (both on-time). The difference in D_e between the 4 and 40–48 s exposures is not significant for two samples and barely significant at one-sigma for the other. In two cases the 4 s exposure produces a slightly higher D_e value, but this is opposite of what might be expected if the 4 s exposure was not fully resetting the signal resulting in build-up of signal as the sequence proceeds and therefore a steeper growth curve. Such build-up might be happening, but if so the test dose seems to correct for it. The shorter exposures do not therefore appear detrimental. This will save considerable machine time in future work, but it is recommended that longer exposures also be employed on a few aliquots to make sure there are no systematic effects.

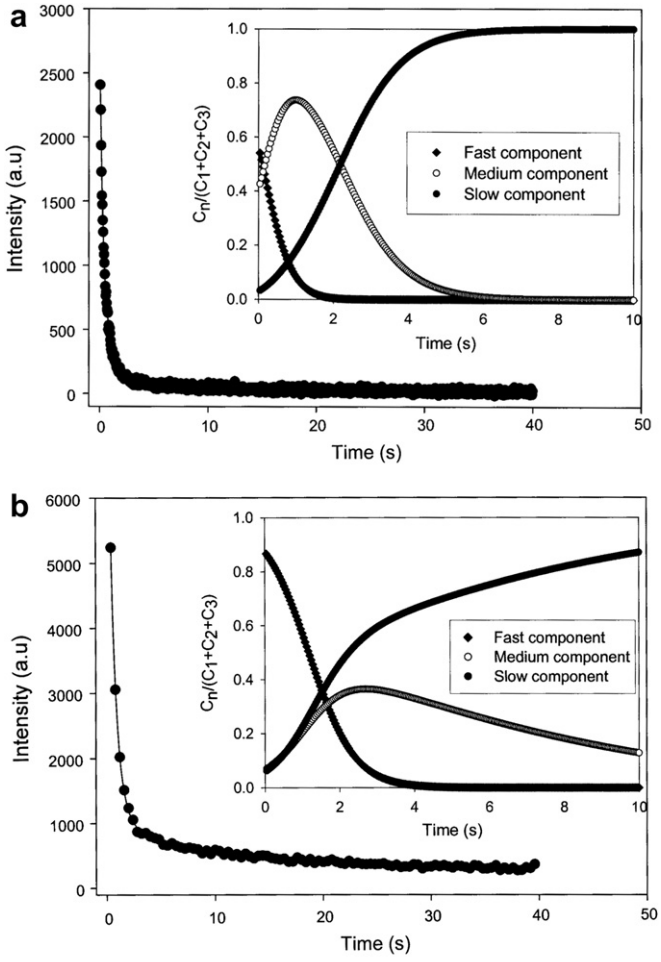

Fig. 4. The time-dependence of luminescence for pulsing (a) and CW optical stimulation (b). The solid line represents a fit using three exponentials. The insets show the relative importance of each component, showing the decrease in time of the fast component, and the change in time of the medium and slow components over the first 10 s.

Further evidence that the 4s exposures are sufficient comes from the dose recovery tests. Aliquots were first exposed to pulsed blue light using either 4 or 40–48 s exposure times and then given an irradiation (between 7.2 and 24 Gy, depending on size of natural D_e). Fig. 3a shows a radial graph of the OSL dose/administered dose ratio for both exposure times. Most aliquots for either exposure are within 2-sigma of 1.0, which is also the case for the CW measurements of both polyminerals (Fig. 3b) and fine quartz extracts. The weighted average of all pulsed dose recovery tests is 0.93 ± 0.06 ($N = 13$) or 1.01 ± 0.04 ($N = 11$) when two outliers are removed. The weighted average for the CW measurements is 0.98 ± 0.03 ($N = 16$) for the polyminerals and 0.98 ± 0.03 for the quartz.

Successful recovery of administered doses of 7.2 Gy, within 2-sigma for all five aliquots measured, and of 2.5 Gy for one aliquot, suggests that thermal transfer for the younger samples may not be a significant problem, although this should require additional study. It is also noted that a recuperated signal after a zero dose (although not a fully sufficient test for lack of thermal transfer) was not observed for most aliquots.

Finally, to judge whether the fast quartz component is removed by the 4 s pulsing exposure, the decay curves shown in Fig. 2 were fitted by the sum of three exponentials (Singarayer and Bailey, 2003; Jain et al., 2003). These fits are shown as a solid line through data points in Fig. 4a for the pulsed data and in Fig. 4b for the CW-OSL data, both on polymineral aliquots. To determine the time-evolution of the fast component, the relevant importance of each component was plotted against the stimulation time as shown in the insets using the method of Chithambo and Galloway (2001).

Table 3
Fading rates expressed as *g*-values (%/decade) for individual aliquots.

Sample	CW IRSL	CW OSL	Pulsed IRSL	Pulsed OSL
UW1691	7.6 ± 0.8	0.8 ± 0.7	3.3 ± 1.3	1.3 ± 0.9
	7.0 ± 1.0	0.7 ± 0.8	-1.9 ± 1.2	0.1 ± 0.6
	6.1 ± 0.8	0.5 ± 0.7	0.3 ± 0.9	0.2 ± 0.6
UW1692	6.2 ± 0.8	1.0 ± 0.8	4.0 ± 1.2	-0.7 ± 0.7
	4.9 ± 0.8	3.6 ± 0.8	3.5 ± 1.1	0.7 ± 0.7
	4.8 ± 0.8	2.6 ± 0.8	1.2 ± 1.0	0.2 ± 0.6
UW1693	6.9 ± 0.8	-0.3 ± 0.8	2.4 ± 1.3	-1.7 ± 0.7
	5.8 ± 0.8	2.0 ± 1.0	2.2 ± 0.9	0.0 ± 0.7
	6.3 ± 0.9		0.0 ± 1.4	-0.4 ± 0.7
	6.9 ± 1.2	4.2 ± 1.8	1.0 ± 3.7	-1.0 ± 1.5
	6.0 ± 1.2	-1.3 ± 1.7	1.7 ± 2.7	-1.0 ± 1.5
	5.0 ± 1.2	0.1 ± 2.0	13.6 ± 4.9	-1.5 ± 1.7
UW1694	7.6 ± 1.1	1.0 ± 2.0	4.5 ± 1.8	-0.4 ± 1.7
	6.0 ± 1.1	5.0 ± 2.0	6.3 ± 1.9	-1.7 ± 1.8
UW1695	5.2 ± 1.1	1.0 ± 2.0	-2.0 ± 2.0	-1.6 ± 1.9
	4.8 ± 1.1	5.0 ± 3.0	-1.3 ± 1.9	-5.0 ± 2.0
	5.2 ± 1.3	6.0 ± 6.2	3.4 ± 3.6	0.5 ± 3.2
	7.6 ± 1.2	8.9 ± 5.2	-0.4 ± 4.5	0.1 ± 3.3
	7.2 ± 1.4	0.7 ± 6.6	7.9 ± 5.7	2.8 ± 3.7
UW1696	4.7 ± 1.0	-1.4 ± 1.2	-3.5 ± 1.2	0.9 ± 0.8
	13.5 ± 0.9	0.3 ± 1.0	-3.5 ± 1.2	0.9 ± 0.8
	4.1 ± 1.8	7.6 ± 3.1	1.1 ± 3.8	-1.8 ± 2.3
	5.2 ± 1.5	1.5 ± 2.8	3.4 ± 4.1	1.9 ± 2.1
	5.7 ± 1.5	3.8 ± 2.8	2.1 ± 4.5	-2.2 ± 2.4
UW1697	5.1 ± 0.9	1.4 ± 0.9	0.0 ± 1.2	-2.7 ± 1.0
	6.7 ± 1.0	1.4 ± 0.8	8.5 ± 1.5	-1.0 ± 1.0
	10.6 ± 1.0	2.5 ± 0.8	7.0 ± 2.0	-1.7 ± 0.8
	7.3 ± 1.1	0.3 ± 0.9	4.0 ± 2.0	-1.0 ± 0.8
UW1698	4.0 ± 1.5	2.2 ± 1.7	-8.0 ± 11	-5.0 ± 2.0
	3.9 ± 1.6	0.7 ± 1.7	21 ± 13	1.0 ± 2.0
	0.1 ± 2.0	-1.8 ± 1.9	7.2 ± 4.8	1.6 ± 2.0
	6.9 ± 1.7	-0.3 ± 2.2	-5.7 ± 4.5	0.5 ± 2.0
	9.6 ± 2.0	2.9 ± 2.9	-1.1 ± 4.8	-2.2 ± 2.2
Weighted average	$\mathbf{6.4 \pm 0.4}$	$\mathbf{1.2 \pm 0.4}$	$\mathbf{1.4 \pm 1.0}$	$\mathbf{-0.3 \pm 0.3}$

Table 4
Equivalent dose values (Gy) using common age/central age models (Galbraith et al., 1999).

OSL									
Sample	CW polymineral			Pulsed			CW quartz		
	N	D_e (Gy)	σ_b (%)	N	D_e (Gy)	σ_b (%)	N	D_e (Gy)	σ_b (%)
UW1691	6	18.6 ± 0.5	4.4 ± 2.6	19	18.6 ± 0.4	7.1 ± 1.9			
UW1692	7	9.1 ± 0.7	19.0 ± 5.5	8	7.2 ± 0.2	4.8 ± 3.2			
UW1693	16	5.3 ± 0.15	9.3 ± 2.3	9	5.2 ± 0.2	5.5 ± 3.7			
UW1694	7	52.9 ± 4.2	0	17	51.8 ± 2.5	13.6 ± 4.3	9	36.2 ± 1.7	12.1 ± 4.0
UW1695	6	36.9 ± 2.9	0	10	48.5 ± 4.3	23.0 ± 7.2	6	47.8 ± 3.0	12.7 ± 5.2
UW1696	11	1.7 ± 0.2	36.2 ± 9.1	11	1.1 ± 0.1	29.1 ± 11.4	6	1.3 ± 0.2	26.6 ± 10.1
UW1697	6	8.6 ± 0.3	5.7 ± 2.8	7	8.2 ± 0.2	0	6	8.1 ± 0.3	8.5 ± 2.9
UW1698	14	2.7 ± 0.2	23.1 ± 5.4	9	2.7 ± 0.3	24.6 ± 7.4	6	2.3 ± 0.6	0.8 ± 4.2
UW1699	4	1.5 ± 0.2	0	7	1.7 ± 0.2	23.5 ± 12.1	6	0.8 ± 0.1	11.2 ± 4.4

IRSL						
Sample	CW polymineral			Pulsed		
	N	D_e (Gy)	σ_b (%)	N	D_e (Gy)	σ_b (%)
UW1691	6	21.4 ± 1.3	13.7 ± 4.7	4	22.4 ± 2.1	14.6 ± 8.0
UW1692	7	6.7 ± 2.0	3.5 ± 4.3	6	7.9 ± 1.4	34.2 ± 13.9
UW1693	16	5.2 ± 0.2	13.0 ± 3.0	3	6.3 ± 1.0	0
UW1694	12	53.9 ± 1.2	3.5 ± 2.6	12	62.2 ± 4.0	20.4 ± 5.0
UW1695	12	45.5 ± 1.1	6.9 ± 2.2	7	48.1 ± 2.5	0
UW1696	12	1.2 ± 0.1	30.6 ± 9.3	1	1.8 ± 1.6	
UW1697	8	6.6 ± 0.4	13.8 ± 5.6	2	7.0 ± 2.2	0
UW1698	13	3.2 ± 0.2	24.1 ± 6.0	2	3.5 ± 0.9	0
UW1699	3	1.4 ± 0.3	0			

Fig. 4a shows that the fast component decreases from an initial proportion of about 52% of the total signal and is virtually depleted in the initial 2 s. In comparison, the fast component in the CW-OSL case is dominant, just over 85% of the initial signal in the initial transient, but is depleted by 4 s after the start of stimulation.

Table 3 gives g-values ($T_c = 2$ days) for various aliquots, representing 8 of the sediment samples, and their weighted average. Almost all the CW-IRSL signals and many of the CW-OSL signals exhibit significant fading, although the OSL fading is not substantial, with a weighted average of 1.2%. For the pulsed OSL, there was no significant fading for the most part. It thus appears that conventional double SAR does not eliminate entirely the possibility of fading of the OSL signal for these samples, but such fading is largely eliminated by the pulsed signal.

The pulsing by itself does not fully eliminate a feldspar signal, which does have a tail extending beyond 10 μs (Clark and Bailiff, 1998; Denby et al., 2006). Of the 97 aliquots from various samples which produced a measurable pulsed signal, 37 produced a pulsed IRSL signal of sufficient quality that an equivalent dose could be obtained. However, as Table 3 shows, fading of this signal was much less substantial than for CW IRSL, and in several cases was not significant at all. Sanderson and Clark (1994) and Tsukamoto et al. (2006) also observed reduced fading for longer lived components (>10 μs) in time resolution studies of coarse-grained feldspars.

Table 4 compares central D_e values for OSL and IRSL in both CW and pulsed mode. The central tendency is determined by the central age model (Galbraith et al., 1999), which also computes over-dispersion values (σ_b). Some samples show considerable inter-aliquot scatter (average errors on individual aliquots were 13% for CW polyminerals, 17% for pulsed polyminerals, and 8% for CW quartz). Overall differences between CW and pulsed and between OSL and IRSL, however, are small, with some exceptions. Before this comparison can be taken at face value, both alpha efficiency and fading must be taken into account.

It has long been appreciated that alpha radiation is more efficient at producing luminescence in feldspars than in quartz (Aitken, 1985: 199). Our laboratory has measured b-values on IRSL and OSL signals for numerous fine-grained ceramic samples and has found that the OSL b-value generally ranges from about 0.4 to 0.8 Gy μm^2, while the IRSL b-value is higher and more variable, typically ranging from 1 to 3. To appreciate the error involved by not taking this into account, using an average quartz b-value versus an average feldspar b-value for a CW-OSL age determination makes as much as a 20% percent difference in age (as calculated for UW1691). If CW-OSL signal contains a feldspar component and the pulsed OSL signal does not, then the b-value should be higher for CW OSL than it is for pulsed and its D_e value, if assuming no fading, should be higher to yield the same age.

Table 5
Average b-values (Gy μm^2).

OSL									
Sample	CW polymineral			Pulsed			CW quartz		
	N	b-value	σ_b (%)	N	b-value	σ_b (%)	N	b-value	σ_b (%)
UW1694-1695	7	1.47 ± 0.22	23.4 ± 14.8	16	0.95 ± 0.09	30.0 ± 8.5	6	0.52 ± 0.03	10.3 ± 5.3
All others	32	0.56 ± 0.02	9.2 ± 2.9	31	0.55 ± 0.03	22.0 ± 4.7	12	0.39 ± 0.01	0.9 ± 7.0

IRSL						
Sample	CW polymineral			Pulsed		
	N	b-value	σ_b (%)	N	b-value	σ_b (%)
All samples	45	1.41 ± 0.05	19.9 ± 2.9	10	1.01 ± 0.10	20.9 ± 7.9

Table 6
Ages (ka).

Sample	Quartz	CW OSL	CW-OSL fading correction	CW IRSL	CW-IRSL fading correction	Pulsed OSL	Pulsed IRSL
UW1691		5.07 ± 0.26	5.36 ± 0.16	4.80 ± 0.36	9.53 ± 0.61	5.08 ± 0.25	5.48 ± 0.59
UW1692		2.76 ± 0.24	3.58 ± 0.27	1.72 ± 0.09	2.75 ± 0.11	2.17 ± 0.12	2.17 ± 0.39
UW1693		1.46 ± 0.08	1.62 ± 0.10	1.20 ± 0.07	1.94 ± 0.06	1.44 ± 0.08	1.56 ± 0.26
UW1694	11.1 ± 0.7	13.2 ± 1.3	23.2 ± 3.59	13.6 ± 0.7	28.0 ± 1.93	14.4 ± 1.0	17.0 ± 1.4
UW1695	18.0 ± 1.4	11.3 ± 1.1	35.2 ± 8.17	14.2 ± 0.7	26.9 ± 1.32	16.6 ± 1.7	16.3 ± 1.2
UW1696	0.41 ± 0.06	0.51 ± 0.06	0.68 ± 0.09	0.31 ± 0.04	0.66 ± 0.10	0.34 ± 0.04	0.49 ± 0.45
UW1697	2.39 ± 0.14	2.41 ± 0.13	3.02 ± 0.13	1.54 ± 0.12	3.07 ± 0.23	2.33 ± 0.11	1.79 ± 0.56
UW1698	0.86 ± 0.05	0.97 ± 0.08	1.11 ± 0.11	0.92 ± 0.08	1.51 ± 0.15	0.97 ± 0.10	1.10 ± 0.28
UW1699	0.32 ± 0.02	0.58 ± 0.06		0.42 ± 0.08		0.66 ± 0.09	

As mentioned, *b*-value was determined in different ways, but no systematic difference was noticed among the methods, so all results are combined, and weighted averages and over-dispersion values (using the central age model of Galbraith et al., 1999) are shown in Table 5. Several observations can be made. First, a systematic and significant difference is present across all methods for the OSL *b*-value between the two oldest samples, UW1694 and UW1695, and all others. In the table the results for those two samples are combined separately from all others. Mauz et al. (2006) also reported high alpha efficiency values for higher dosed quartz samples. This difference did not extend to IRSL (where results from all samples are combined). Second, there was no difference in *b*-value between 4 s and 40–48 s exposures for pulsed OSL for UW1691 (0.50 ± 0.03 for 4 s, 0.49 ± 0.05 for 40–48 s), but there was for UW1694 (1.20 ± 0.10 for 4 s, 0.63 ± 0.07 for 40–48 s). We do not have a good explanation for this. (The only other sample measured with longer exposures, UW1699, yielded no measurable *b*-value data with the longer exposures.)

Third, the difference in *b*-value between CW OSL for polyminerals and pulsed OSL is minimal for all samples except UW1694 and UW1695. There is also a significant difference between CW and pulsed IRSL. The latter, however, may partly reflect the fact that seven of the 10 pulsed IRSL values are from UW1694 and UW1695. Finally, the *b*-values for the fine quartz extracts are significantly lower than all other results. These values of 0.4–0.5 correspond to *a*-values (an alternative measure of alpha efficiency) of about 0.03–0.04, which is within the range reported for quartz by Lai et al. (2008) and Mauz et al. (2006). The higher *b*-values in the pulsed OSL may reflect what was mentioned in regard to fading, that the pulsing does not eliminate the feldspar signal (thus the higher b-value), but rather greatly reduces a fading signal.

Computed ages are given in Table 6. For the CW data, ages are given both uncorrected and corrected for fading (Huntley and Lamothe, 2001). For the corrected ages, an average *g*-value for the sample was used. This was justified on the basis that little correlation between *g*-value and D_e was found for most samples (Buylaert et al., 2008). There was some correlation (>0.35 R^2) for a few samples (4 out of 16 comparisons of either OSL or IRSL), but on these samples using an average *g*-value for all D_e values to produce ages and using the average age only for those aliquots where fading was measured made no significant difference.

Fig. 5 compares the fading-corrected polymineral CW and the pulsed OSL ages with the ages from the extracted quartz. The pulsed OSL ages are in statistical agreement, at 1-sigma, with the quartz ages for four of six samples. For CW OSL none are in statistical agreement with the quartz. All in fact are older. The pulsed IRSL ages (not shown in the figure) are in statistical agreement with the pulsed OSL for eight of nine samples and with the quartz for 4 of 5 samples. The fading-corrected CW-IRSL ages also do not agree with the quartz ages and are for the most part older than the fading-corrected CW-OSL ages (one is younger).

An explanation for the older CW ages is that the feldspar signal was not as well bleached at deposition as the quartz signal. Feldspar is known to bleach at a slower rate (Godfrey-Smith et al., 1988; Thomsen et al., 2008b). This would also explain the older CW-OSL ages because they have retained some feldspar signal, as the fading data also suggest. This raises doubts that the ages reflect loess deposition, which normally produces well-bleached sediments (Roberts, 2008).

The older ages for the two pulsed OSL results that did not agree with the quartz ages (UW1694 and UW1699) are more difficult to explain because at least UW1694 did not show any fading. No

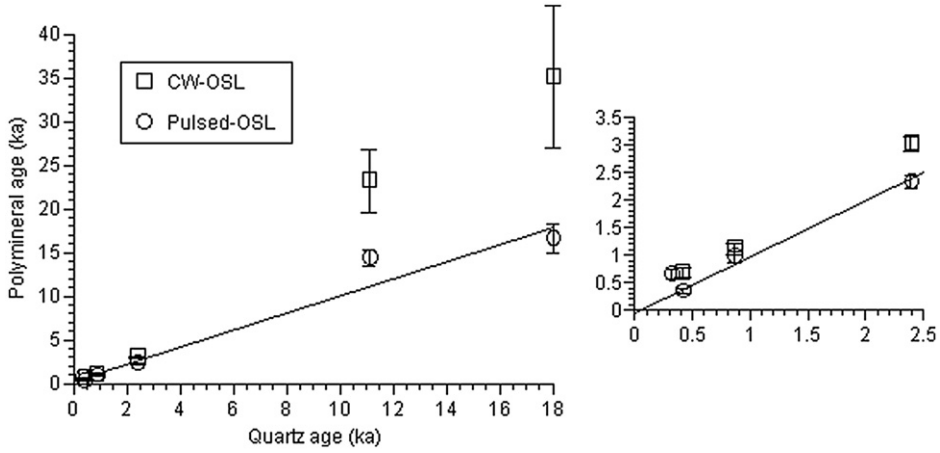

Fig. 5. Comparison of age determinations per sample between those from quartz OSL and those from polymineral OSL, either CW or pulsed mode. The insert shows the lower values in more detail.

fading test was conducted on UW1699, partly because the pulsed OSL signal from this young sample was very weak, the weakest of all the samples. The significantly older age for this sample might just reflect underestimation of error. UW1694 is more of a puzzle. It is stratigraphically below UW1695, for which the pulsed OSL and the quartz ages are in agreement. The pulsed ages for UW1694 and UW1695 are statistically indistinguishable, but the quartz OSL age and the CW-OSL age for UW1694 are both younger than that for UW1695, putting it out of stratigraphic order. No good explanation is apparent, possibly an error in dose rate.

Otherwise, the ages increase with depth and are in correct stratigraphic order. The current favored hypothesis that these terracettes formed by slumping as a result of rotational agricultural practices (Henck et al., 2010) is thus supported in this sense. However, the hypothesis does not predict poor bleaching, which might suggest an alternative explanation, mainly that the dates are addressing colluvial events that formed the terracettes, allowing sufficient exposure to reset the quartz signal but less so the feldspar signal. However, while landslide debris is apparent in some of the terracettes, it is distinct from the loess-like silt forming the bulk of the stratigraphy.

The only independent age controls are from four radiocarbon assays on charcoal, which range in age from 1400 to 2400 years ago (calibrated). None of the samples used in the assays were taken from exactly the same place as the OSL samples and the events dated by either method may not be well associated. Nonetheless, most of the OSL dates are in the same range as those from radiocarbon. This also suggests the OSL dates may not be addressing original deposition. The two exceptions are UW1694 and UW1695, both of which give a Pleistocene age, and thus are addressing a much earlier event. UW1695, curiously, is the only sample associated with a paleosol.

5. Conclusions

In hindsight, these particular samples were probably not the best for demonstrating the advantages of pulsed over CW OSL for dating. If the CW-OSL ages were taken at face value, i.e., not corrected for anomalous fading, the results, when compared to those from the quartz extracts, are nearly as good as those from pulsed OSL (Table 6). This is because the samples appear to be partially bleached, which off-sets the fading. It is only when fading is taken into account that the CW-OSL results are systematically in error. This shows that the double SAR method in CW mode is not sufficient for removing a fading component from OSL, but pulsed OSL is. The evidence, from the pulsed IRSL signal and from the *b*-value measurements, also shows that pulsed OSL does not eliminate a feldspar signal in double SAR, although it does reduce it, but it does reduce a significant fading component. The pulsed IRSL also showed reduced fading.

Using the double SAR method in both CW and pulsed mode and consideration of fading allowed the detection of partial bleaching in fine grains, by distinguishing quartz and feldspar signals. The fact that the samples are poorly bleached questions whether the ages are addressing original aeolian deposition. Rather they seem to be addressing some colluvial event responsible for the terracette formations, although a mechanism apart from slumping is not apparent from the geological evidence.

Acknowledgments

Funding for the pulsed equipment was made possible by the University of Washington Student Technology Fund. The research benefitted from experimental work by and advice from Christina Ankjaergaard.

References

Aitken, M.J., 1985. Thermoluminescence Dating. Academic Press, London.
Ankjaergaard, C., Jain, M., Thomsen, K.J., Murray, A.S., 2010. Optimising the separation of quartz and feldspar optically stimulated luminescence using pulsed excitation. Radiation Measurements 45, 778–785.
Auclair, M., Lamothe, M., Huot, S., 2003. Measurement of anomalous fading for feldspar IRSL using SAR. Radiation Measurements 37, 487–492.
Bailiff, I.K., Mikhailik, V.B., 2003. Spatially-resolved measurement of optically stimulated luminescence and time-resolved luminescence. Radiation Measurements 37, 151–159.
Banerjee, D., Murray, A.S., Bøtter-Jensen, L., Lang, A., 2001. Equivalent dose estimation using a single aliquot of polymineral fine grains. Radiation Measurements 33, 73–94.
Buylaert, J.P., Murray, A.S., Huot, S., 2008. Optical dating of an Eemian site in northern Russia using K-feldspar. Radiation Measurements 43, 715–720.
Chithambo, M.L., 2007a. The analysis of time-resolved optically stimulated luminescence. I. Theoretical considerations. Journal of Physics D: Applied Physics 40, 1874–1879.
Chithambo, M.L., 2007b. The analysis of time-resolved optically stimulated luminescence. II. Computer simulations and experimental results. Journal of Physics D: Applied Physics 40, 1880–1889.
Chithambo, M.L., Galloway, R.B., 2001. On the slow component of OSL stimulated from quartz by pulsed blue light emitting diodes. Nuclear Instruments and Methods B 183, 358–368.
Clark, R.J., Bailiff, I.K., 1998. Fast time-resolved luminescence emission spectroscopy in some feldspars. Radiation Measurements 29, 553–560.
Clark, R.J., Bailiff, I.K., Tooley, M.J., 1997. A preliminary study of time resolved luminescence in some feldspars. Radiation Measurements 27, 211–220.
Denby, P.M., Bøtter-Jensen, L., Murray, A.S., Thomsen, K.J., Moska, P., 2006. Applications of pulsed OSL to the separation of the luminescence components from a mixed quartz/feldspar sample. Radiation Measurements 41, 774–779.
Duller, G.A.T., Bøtter-Jensen, L., 1993. Luminescence from potassium feldspars stimulated by infrared and green light. Radiation Protection Dosimetry 47, 683–688.
Galbraith, R.F., Roberts, R.G., Laslett, G.M., Yoshida, H., Olley, J.M., 1999. Optical dating of single and multiple grains of quartz from Jinmium rock shelter, northern Australia. Part I. Experimental design and statistical models. Archaeometry 41, 339–364.
Godfrey-Smith, D.I., Huntley, D.J., Chen, W.H., 1988. Optically dating studies of quartz and feldspar sediment extracts. Quaternary Science Reviews 7, 373–380.
Henck, A., Taylor, J., Lu, H., Li, Y., Yang, Q., Grub, B., Breslow, S.J., Robbins, A., Elliott, A., Hinckley, T., Combs, J., Urgenson, L., Widder, S., Hu, X., Ma, Z., Yuan, Y., Jian, D., Liao, X., Tang, Y., 2010. Anthropogenic hillslope terraces and swidden agriculture in Jiuzhaigou National Park, northern Sichuan, China. Quaternary Research 73, 201–207.
Huntley, D.J., Berger, G.W., Bowman, S.G.E., 1988. Thermoluminescence responses to alpha and beta irradiations, and age determination when the high dose response is non-linear. Radiation Effects 105, 279–284.
Huntley, D.J., Lamothe, M., 2001. Ubiquity of anomalous fading in K-feldspars and the measurements and correction for it in optical dating. Canadian Journal of Earth Science 38, 1093–1106.
Jain, M., Murray, A.S., Bøtter-Jensen, L., 2003. Characterization of blue-light stimulated luminescence components in different quartz samples: implications for dose measurements. Radiation Measurements 37, 441–449.
Kortekaas, M., Murray, A.S., 2005. A method for the removal of micas from quartz separates. Ancient TL 23, 43–46.
Lai, Z-P., Zoller, L., Fuchs, M., Bruckner, H., 2008. Alpha efficiency determination for OSL of quartz extracted from Chinese loess. Radiation Measurements 43, 767–770.
Mauz, B., Packman, S., Lang, A., 2006. The alpha effectiveness in silt-sized quartz: new data obtained by single and multiple aliquot protocols. Ancient TL 24, 47–52.
Murray, A.S., Wintle, A.G., 2000. Luminescence dating of quartz using an improved single-aliquot regenerative-dose protocol. Radiation Measurements 32, 57–73.
Roberts, H.M., 2007. Assessing the effectiveness of the double-SAR protocol in isolating a luminescence signal dominated by quartz. Radiation Measurements 42, 1627–1636.
Roberts, H.M., 2008. The development and application of luminescence dating to loess deposits: a perspective on the past, present and future. Boreas 37, 483–507.
Roberts, H.M., Wintle, A.G., 2001. Equivalent dose determinations for polymineralic fine-grains using the SAR protocol: applications to a Holocene sequence of the Chinese Loess Plateau. Quaternary Science Reviews 20, 859–863.
Sanderson, D.C.W., Clark, R.J., 1994. Pulsed photostimulated luminescence of alkali feldspars. Radiation Measurements 23, 633–639.
Singarayer, J.S., Bailey, R.M., 2003. Further investigations of the quartz optically stimulated luminescence components using the linear modulation. Radiation Measurements 37, 451–458.
Thomsen, K.J., Bøtter-Jensen, L., Denby, P.M., Moska, P., Murray, A.S., 2006. Developments in luminescence measurement techniques. Radiation Measurements 41, 768–773.
Thomsen, K.J., Jain, M., Murray, A.S., Denby, P.M., Roy, N., Bøtter-Jensen, L., 2008a. Minimizing feldspar OSL contamination in quartz UV-OSL using pulsed blue stimulation. Radiation Measurements 43, 752–757.

Thomsen, K.J., Murray, A.S., Jain, M., Botter-Jensen, L., 2008b. Laboratory fading rates of various luminescence signals from feldspar-rich sediment extracts. Radiation Measurements 43, 1474–1486.
Tsukamoto, S., Denby, P.M., Murray, A.S., Bøtter-Jensen, L., 2006. Time-resolved luminescence from feldspars: new insight into fading. Radiation Measurements 41, 790–795.
Vincent, P.J., Clarke, J.V., 1979. The terracette enigma – a review. Biuletyn Peryglacjalny 25, 65–77.
Visocekas, R., 1988. Comparison between tunneling afterglows following alpha or beta irradiations. Nuclear Tracks and Radiation Measurements 14, 163–168.
Zhang, J.F., Zhou, L.P., 2007. Optimization of the 'double SAR' procedure for polymineral fine grains. Radiation Measurements 42, 1475–1482.
Zimmerman, D.W., 1967. Thermoluminescence from fine grains from ancient pottery. Archaeometry 10, 26–28.